



Comparing MODIS daily snow albedo to spectral albedo field measurements in Central Greenland



Patrick Wright^{a,*}, Mike Bergin^b, Jack Dibb^c, Barry Lefer^a, Florent Domine^d, Tobey Carman^e, Carlo Carmagnola^f, Marie Dumont^f, Zoe Courville^g, Crystal Schaaf^h, Zhuosen Wang^h

^a Department of Earth and Atmospheric Sciences, University of Houston, 312 SR1, Houston, TX 77204, United States

^b School of Civil and Environmental Engineering, School of Earth and Atmospheric Science, Georgia Tech, 311 Ferst Drive, Atlanta, GA 30332, United States

^c Institute for the Study of Earth, Oceans, and Space, University of New Hampshire, Morse Hall, 8 College Road, Durham, NH 03824-352, United States

^d Takuvik International Laboratory, Université Laval and CNRS, Pavillon Alexandre Vachon, 1045 avenue de La Médecine, Québec, QC, G1V 0A6, Canada

^e Department of Computer Science, University of Alaska Fairbanks, 513 Ambler Lane, Chapman Building, RM 202, Fairbanks, AK 99775-6670, United States

^f Snow Research Center, Meteo-France/CNRS/CNRM-GAME, 1441 rue de la Piscine, 38400 St. Martin d'Heres, France

^g U.S. Army Cold Regions Research and Engineering Laboratory (CRREL), 72 Lyme Rd., Hanover, NH 03755, United States

^h Environmental Earth and Ocean Sciences, University of Massachusetts Boston, 100 Morrissey Blvd, Boston MA 02125, United States

ARTICLE INFO

Article history:

Received 4 November 2012

Received in revised form 26 August 2013

Accepted 27 August 2013

Available online xxxx

Keywords:

MODIS

Snow albedo

Summit

Greenland

ABSTRACT

The albedo of the Greenland ice sheet plays a key role in the energy balance and climate of the arctic. Change in snow albedo values associated with changing climate conditions can be monitored remotely from satellite platforms viewing the entire Greenland ice sheet, yet comparisons to high quality surface measurements are necessary to assess the accuracy of satellite measurements as new snow albedo algorithms are developed with higher spatial and temporal resolution.

During May, June, and July 2011, we obtained daily measurements of spectral albedo at Summit, Greenland with an Analytical Spectral Devices (ASD) spectroradiometer, scanning at 350–2200 nm. We compare our spectral albedo field measurements to the Moderate Resolution Imaging Spectrometer (MODIS), using both the Version 005 Direct Broadcast daily albedo product and the recently developed Version 006 MCD43A daily albedo product. The spectral field measurements allow calculation of weighted integrals to compare to seven MODIS narrow bandwidths ranging the UV through Infrared, as well as a broadband integration to compare to the MODIS shortwave albedo. We additionally compare our field measurements to albedo measured at the Baseline Surface Radiation Network (BSRN) station at Summit.

Using the MODIS Version 005 Direct Broadcast product, high-quality retrievals only, comparison to field measurements results in root mean square error (RMSE) of 0.033 for the MODIS shortwave product, and RMSE for the MODIS narrow bandwidths ranging 0.022–0.077. The new MODIS Version 006 product shows considerable improvement, with shortwave RMSE of 0.026, and narrow bandwidths ranging 0.020–0.048. These error values for the Version 006 albedo product show an improvement in reported error values from previous MODIS field validations in Greenland, which have been limited to broadband data from the Greenland Climate Network Automatic Weather Stations.

© 2013 Elsevier Inc. All rights reserved.

1. Introduction

Surface albedo is a key parameter that defines the amount of solar radiation absorbed at earth's surface. Accurate snow albedo measurements are needed to estimate direct radiative forcing by both aerosols and clouds, as well as to assess long term changes in planetary albedo, which will be among the most powerful feedback processes in the

response of the climate system to anthropogenic forcing (Donohoe & Battisti, 2011). Satellite platforms are extremely valuable tools to measure surface albedo over very large areas, yet there must be robust comparisons to high-quality surface measurements to evaluate algorithms that produce albedo data from remote measurements of directional radiance.

In this study, we focus on a comparison of our spectral albedo measurements to the Moderate Resolution Imaging Spectrometer (MODIS), using the Version 005 (v005) Direct Broadcast daily albedo product and the recently developed Version 006 (v006) MCD43A daily albedo product. Both these products use Terra and Aqua v005 MODIS surface reflectance inputs. Field albedo measurements at Summit Station were made with an Analytical Spectral Devices (ASD) spectroradiometer at

* Corresponding author. Tel.: +1 713 743 3399; fax: +1 713 748 7906.

E-mail addresses: patrickjwright@gmail.com (P. Wright), michael.bergin@ce.gatech.edu (M. Bergin), jack.dibb@unh.edu (J. Dibb), florent.domine@takuvik.ulaval.ca (F. Domine), uaf-cs-dept@alaska.edu (T. Carman), carlo.carmagnola@meteo.fr (C. Carmagnola), marie.dumont@meteo.fr (M. Dumont), Zoe.R.Courville@usace.army.mil (Z. Courville), crystal.schaaf@umb.edu (C. Schaaf), zhuosen.wang@umb.edu (Z. Wang).

350–2200 nm. We do not present data from snow properties measurements in this study, but we reference results from a related modeling study (Carmagnola et al., 2013) to discuss the variability present in both MODIS and ASD field-measured albedo. Additionally, we compare both the ASD field measurements and the MODIS albedo results to albedo measured at the Baseline Surface Radiation Network (BSRN) at Summit.

Many previous validations of MODIS albedo for the Greenland ice sheet (i.e. Liang, Stroeve, & Box, 2005; Stroeve et al., 2005; Stroeve, Box, & Haran, 2006) almost exclusively utilize surface data from the Greenland Climate Network Automatic Weather Stations (GCNet AWS) (Steffen, Box, & Abdalati, 1996). Most recently, Box et al. (2012) present albedo data using the MOD10A1 daily albedo product for the June–August period of 2000–2011, showing a significant albedo decline over the entire Greenland ice sheet (-0.056 ± 0.007), and an albedo decline of -0.046 ± 0.006 for the accumulation zone around Summit over the same period. The authors evaluate the MODIS measurements through comparison with monthly mean albedo measured at GCNet stations, and conclude that the MOD10A1 albedo product is accurate in representing Greenland ice sheet albedo with Root Mean Square Error (RMSE) of 0.041 ± 0.011 .

In this study we provide considerable support to validation efforts and conclusions such as those presented in Box et al. (2012), by providing a comparison that is independent of the GCNet AWS. There are multiple problems that can affect unattended radiation stations such as the GCNet AWS, with poor instrument level and sensor riming likely being the most significant. Additionally, most previous MODIS albedo validations, including studies outside of Greenland (i.e. Liu et al., 2009; Painter et al., 2009), use field measurements from shortwave broadband pyranometers. In this study we compare to high resolution spectral measurements, allowing independent comparison to each of the MODIS narrowbands in addition to the broadband shortwave product.

As part of the Summit 2011 campaign, properties of the snow surface at Summit were measured daily, with the goal of demonstrating the impact of snow grain size and snow chemistry on the temporal variability of albedo (Carmagnola et al., 2013). Snow grain size was measured as specific surface area (SSA, m^2/kg), using a Dual Frequency Integrating Sphere (DUFISSS) operating at 1310 nm (Gallet, Domine, Zender, & Picard, 2009). SSA is equivalent to the optical grain radius, and is given by:

$$\text{SSA} = \frac{\text{surface area}}{\text{volume}(\rho_{\text{ice}})} = \frac{3}{r(\rho_{\text{ice}})}, \quad (1)$$

where r is the optical grain radius, and ρ_{ice} is the density of ice. Modeling results presented in Carmagnola et al. (2013) reproduce daily snow albedo using snow SSA and snow chemistry measurements as input to the DISORT code (DIScrete Ordinate Radiative Transfer), and are referenced in this study to analyze the effects of physical snow properties on both field-measured and satellite-derived albedo data.

2. Methods

2.1. MODIS daily snow albedo products

The MODIS instrument is on both the Terra and Aqua satellites, measuring emitted terrestrial radiation with 10–14 passes per day over central Greenland. This study uses 500-meter resolution narrowband and broadband data from two recently developed MODIS daily albedo products: the Direct Broadcast daily albedo operating on Collection Version 005 (v005) surface reflectances (MO/YD09, Vermote, El Saleous, & Justice, 2002; Vermote & El Saleous, 2006, chap. 8), and the new Collection Version 006 (v006) MCD43A daily albedo algorithm (also running on the v005 surface reflectances). Albedo data were computed for 1100 AM local time (to coincide with the timing of field measurements), and for the

specific coordinates of the field site. The bandwidths for the seven MODIS narrowbands and the broadband product used in this study are shown in Table 1.

The Bidirectional Reflectance Distribution Function (BRDF) specifies the angular distribution of surface scattering as a function of illumination and viewing geometries at a particular wavelength. The MODIS Direct Broadcast version of the BRDF/Albedo algorithm uses multiple clear sky surface reflectances from both Terra and Aqua over a 16-day period to reconstruct a generalized BRDF, with observations on a single day emphasized to enable retrieval of a daily value. Integration of the BRDF over all view angles for a particular solar zenith angle provides a measure of black sky albedo with integration over all solar zenith angles providing a measure of white sky albedo (Lucht, Schaaf, & Strahler, 2000; Schaaf et al., 2002). When sufficient observations distributed across the viewing hemisphere are not available, a magnitude inversion (backup algorithm) is used to produce a lower quality daily albedo (color indicated in all figures).

The v006 MODIS albedo product similarly uses multiple clear sky views available over a 16-day period to provide daily albedo values. This includes as many overpasses as are available per day (while earlier versions of the algorithm, including the Direct Broadcast version, were limited to only 4 observations per day). Therefore, the v006 product attempts to better capture daily albedo with an algorithm that more strongly emphasizes all contributions from the single day of interest.

The two data sets were converted from “white-sky” albedo (bihemispherical reflectance under isotropic illumination) and “black-sky” albedo (directional hemispherical reflectance at a particular solar zenith angle) to “blue-sky” albedo, which includes the effects of anisotropic diffuse illumination and multiple scattering between the surface and atmosphere, using clean atmosphere aerosol optical depths (AODs) (Román et al., 2010). At Summit, clean atmosphere AODs are typically near 0.04 for 500 nm. When conditions permitted, these AODs were retrieved from handheld sunphotometers at Summit Station, otherwise they were developed from clear sky MODTRAN simulations for the elevation at Summit (assuming an AOD of 0.1 at sea level). However, it is noted that for clear sky conditions and low to moderate solar zenith angles, variation in AODs will have little effect on these results. The conversion from MODIS narrowbands to a broadband value (0.3–5 μm) is based on the coefficients for high albedo snow given in Stroeve et al., 2005. Both products have a stated accuracy for snow of 5% or less for high-quality only retrievals (Liu et al., 2009).

2.2. Field measurements and instrumentation

2.2.1. ASD spectroradiometer

Spectral albedo was measured at 350–2200 nm with an Analytical Spectral Devices (ASD) Fieldspec Pro spectroradiometer (2001 model), using the ASD Remote Cosine Receptor (RCR) foreoptic. The cosine receptor was mounted on a 109 cm aluminum arm and held level at approximately 90 cm height by sighting a level bubble on the arm. At this height the cosine receptor has approximately a 2-meter radius field of view for 90% of the signal. Four consecutive albedo measurements were made at every location, enabling an analysis of the precision of the manual leveling technique. This method was found to be more rapid and mobile than the use of a tripod mount, enabling measurements at multiple locations during short time periods (limited by computer electronics in very cold temperatures).

The ASD has 3 nm spectral resolution on the visible/near infrared detector (350–1050 nm, silicon photodiode array), and 10–12 nm resolution on the short wave infrared detectors (900–2500 nm, InGaAs). Measurements are made by standing “down-sun” of the receptor, taking consecutive scans of downwelling and upwelling radiation, with 40 measurements and 20 dark currents per scan. Because consecutive measurements are used in ratio to each other in the albedo calculation, irradiance calibration is not applied (instrument last calibrated in 2007).

Table 1
Bandwidths (nm) for the MODIS shortwave and narrowband albedo products.

Shortwave	Band 3	Band 4	Band 1	Band 2	Band 5	Band 6	Band 7
300–5000	459–479	545–565	620–670	841–876	1230–1250	1628–1652	2105–2155

2.2.2. Daily albedo measurements and MODIS pixel locations

Albedo was measured every day with the ASD at 1100 AM local time (1300 GMT) between May 16 and July 19, 2011. Solar zenith angle (SZA) at the time of measurement ranged from 56° on May 16, to 50.7° at the solstice, and returned to 53.4° on July 19. These SZA values are well under the recommended limit of 70° for MODIS product use, and MODIS quality flags, which account for periods of cloudiness and high SZA (Schaaf, Wang, & Strahler, 2011), are clearly indicated in all plots and analyses.

Albedo measurements were made at four fixed sites, each marked with bamboo and separated by 4–6 m, located ~1 km east of the Temporary Atmospheric Watch Observatory (TAWO) building in the clean snow sector at Summit Station (Fig. 1). The spacing of these sites was chosen to sample the approximate visual scale of variability between drifted and scoured features that were observed during the campaign. Additionally, measurements were made at a fifth “roving” site where profiles of snow specific surface area and density were made in the same spot directly after the albedo measurement, and snow chemistry samples were taken nearby. The roving site was continually moving into clean snow, approaching a distance of 600–700 m from the fixed sites by the end of the campaign. This method allows us to monitor the temporal change (day to day) in albedo at the four fixed locations, which can then be compared to the albedo at the roving site where simultaneous changes in snow properties are known.

We compare the average albedo from the four fixed sites to the 500-meter resolution MODIS albedo pixel centered on the coordinates of this location. In addition, six MODIS pixels immediately adjacent to the

south in the clean air sector are compared to analyze for any possible artificial contamination to the signal at our fixed site, and to provide constraints on the spatial variability of the MODIS signal (Fig. 1, pixels N1–N3, S1–S3). The albedo data for the MODIS pixel containing the fixed measurement sites was found to be very similar in trend and magnitude to adjacent MODIS pixels, with no obvious signs of artificial impacts due to small features such as walking paths or bamboo flags.

Measurements of the fraction of diffuse and direct irradiance were made by taking a ratio of consecutive downwelling measurements, using a small cardboard disc on a bamboo pole to shade the receptor from direct light on alternate measurements. These measurements were necessary as inputs to the DISORT code for the albedo modeling efforts presented in Carmagnola et al. (2013).

In addition to the daily surveys, two spatial transect surveys analyzed km-scale albedo variability on May 17 and June 8, taking measurements every 50 m moving approximately 1.5 km east along the clean air sector boundary flag line. We use these surveys to compare the spatial variability represented at the fixed measurement site to the variability represented across the longer transects, and to aid in analysis of field-measured albedo and MODIS albedo, considering the much larger 500 m² field of view used by MODIS.

2.3. BSRN station at Summit

In addition to comparing the MODIS albedo products to ASD-measured spectral albedo, we compare to broadband albedo measured at the Baseline Surface Radiation Network (BSRN) site at Summit,

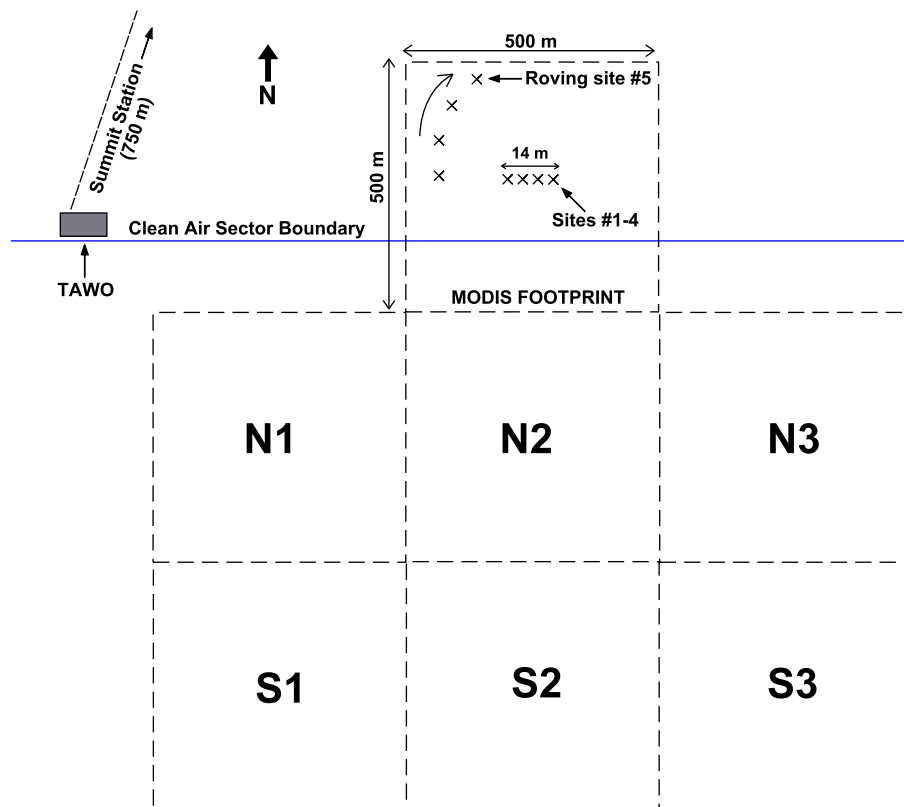


Fig. 1. Map of the field site at Summit, Greenland, showing the fixed and roving albedo sites and the MODIS pixels used in this study.

selecting measurements for 1100 local time from 1-minute resolution data. The BSRN measures downwelling and reflected irradiance with Kipp & Zonen CM21 pyranometers in the range 305–2800 nm (50% transmittance points), or 335–2200 nm (95% transmittance points), with a maximum reported error of 2% for both hourly and daily totals. These instruments are compliant with ISO 9060 (1990) standards of the World Meteorological Organization (WMO).

2.4. Narrowband and broadband albedo calculations

To compare our measured spectral albedo to the MODIS bandwidths, and to the spectral ranges of the BSRN pyranometers, the spectral measurements are integrated over a defined bandwidth, and weighted by the downwelling irradiance. The weighted integral is given by

$$\alpha_{\text{broadband}} = \frac{\int_{\lambda_1}^{\lambda_2} \alpha_{\lambda} F_{\lambda}^{\downarrow} d\lambda}{\int_{\lambda_1}^{\lambda_2} F_{\lambda}^{\downarrow} d\lambda}, \quad (2)$$

where α_{λ} is the spectral albedo, and F_{λ}^{\downarrow} is the spectral downwelling irradiance. Because the ASD spectroradiometer was not calibrated for downwelling irradiance measurements, we have used a radiative transfer model (SBDART) to determine F_{λ}^{\downarrow} between 350 and 2200 nm for each day of the campaign at the time of our measurements. Averages of measurements of atmospheric parameters at Summit during the campaign period, coinciding with the time of daily albedo measurements, were used as model inputs. We used 0.088 Aerosol Optical Thickness at 500 nm, pressure of 680 mb, air temperature of -14 °C, relative humidity of 65%, total water vapor column of 0.03 and total ozone column of 332 Dobson units. We then compared the model results to measurements from a Biospherical Instruments (BSI) SUV-150B scanning spectroradiometer, at 350–600 nm (0.64 nm resolution, cosine-corrected), located on the roof of the Green House building at Summit, approximately 1 km from the measurement site. Any modeled spectra that had RMSE >0.04 W/m²/nm were fitted to the BSI spectra by adjusting cloud optical depth on overcast days (that is, finding the cloud optical depth that provides the best fit between the BSI spectra and SBDART results). For clear sky days where the average parameters cited above did not give a satisfying fit with the BSI spectra, typically the cases for which the modeled spectra was smaller than measurements, the humidity and ozone column values were changed to provide the best fit between the two spectra. Overall, the model matched the measurements very well, with only 3 days out of 52 showing RMSE >0.04 W/m²/nm. These 3 days are the only days for which we needed to adjust the ozone and humidity values. Fig. 2 shows the seven MODIS bandwidths with a typical clear-sky spectral albedo measurement, and the SBDART modeled clear-sky downwelling irradiance

spectrum, where the shape of the downwelling curve over the bandwidth dictates the albedo weighting.

2.5. Albedo corrections and quality control procedure

2.5.1. Shadow corrections

Although the ASD operator stands “down-sun” of the receptor to minimize any direct shadowing effects, there is still a shadow produced in the diffuse light field due to the operator. This causes a reduction in the ASD signal for both downwelling and upwelling measurements, thus requiring a calculation of the solid angle of the cosine response volume that is affected by the operator, and a correction factor to increase the measured response (Grenfell, Warren, & Mullen, 1994).

For clear sky measurements, upwelling reflected radiation is assumed completely diffuse and isotropic, whereas the downwelling has both diffuse and direct components. The measured diffuse fraction of clear-sky downwelling radiation varies with wavelength and is exponentially reduced from ~50% in the UV to almost entirely direct-beam in the long-wave visible and throughout the infrared. Therefore, shadow corrections must be applied independently to the upwelling and downwelling components of diffuse radiation, each calculated as:

$$C_{\text{shadow}\uparrow,\downarrow} = \left(\int_0^{\phi} \int_{\theta}^{\pi/2} \sin\theta \cos\theta d\theta d\phi \right) (1/\pi), \quad (3)$$

where θ and ϕ are defined by the geometries shown in Fig. 3. The shadow corrections are then applied to the albedo calculation as:

$$\alpha_{\lambda,\text{corrected}} = \frac{C_{\text{shadow}\uparrow} F_{\lambda(\text{diffuse})\uparrow}}{C_{\text{shadow}\downarrow} F_{\lambda(\text{diffuse})\downarrow} + F_{\lambda(\text{direct})\downarrow}} \quad (4)$$

In addition to the diffuse shadow due to the operator, the projected direct shadow of the instrumentation (aluminum arm + cosine receptor) was also included in the calculation of the correction factor for the upwelling component. The correction factors are 1/(1 - 0.0155) for the downwelling component, and 1/(1 - 0.0131) for the upwelling component (both assumed constant with wavelength), resulting in an approximately 1% increase in the measured albedo spectrum. Shadow corrections were not applied to days with consistent overcast conditions, where it is assumed that the diffuse shadow of the upper and lower body approximately offset each other.

2.5.2. Cosine response corrections

The response of the ASD RCR receptor deviates slightly from a true cosine response, and corrections for this error should be applied to both the diffuse and direct components. Recent work in Carmagnola et al. (2013) characterized the cosine response of the RCR receptor

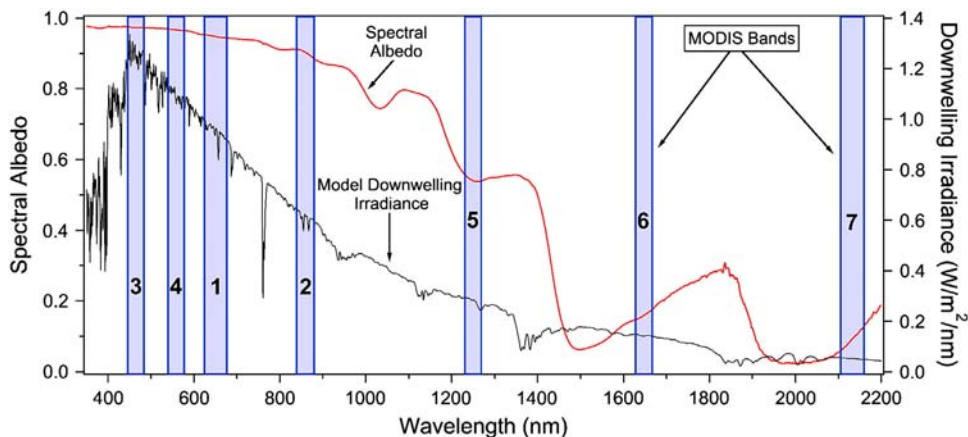


Fig. 2. MODIS bandwidths shown with a typical clear-sky albedo measurement, and a model downwelling irradiance spectrum (SBDART).

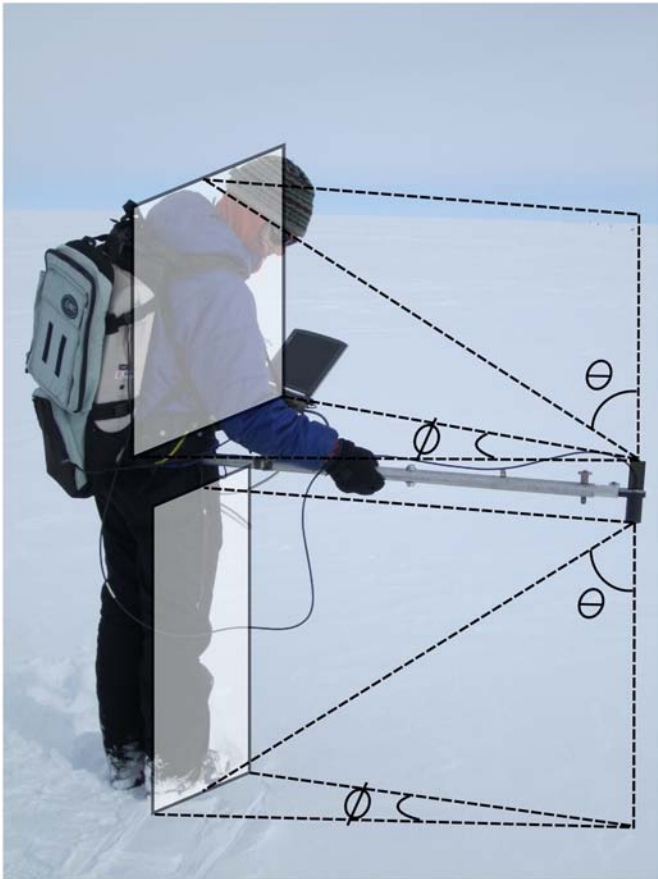


Fig. 3. Geometries used for calculating the correction due to the shadow of the operator in the diffuse light field.

used in our field work in order to quantify the impact on measured fluxes. The RCR was mounted on an optical table in the lab, allowing intensity measurements varying from -90° to $+90^\circ$ with respect to a fixed light source. Results from this work show that cosine corrections increase albedo results by about 1% in the visible, with negligible corrections elsewhere in the measured spectrum. Because this correction is not large enough to significantly affect our results, we have not implemented this correction to our data, however readers should reference Carmagnola et al. (2013) for details regarding methods of the lab routine and cosine correction calculations.

2.5.3. Measured albedo quality control procedure

The discontinuities present in the final dataset of measured albedo are a result of eliminating data that was determined to be of poor quality. Other than instrument failure in extremely cold or windy conditions, poor data were predominantly a result of inconsistent lighting conditions resulting from passing clouds on days that were not entirely clear or entirely overcast.

Albedo spectra were removed from the dataset that: 1) plotted >1.0 in the UV/visible; 2) were obvious outliers from the remaining measurements for a site, that otherwise showed high repeatability; and 3) displayed “parabolic” instrumental error on the VNIR detector (<976 nm). The parabolic error problem has been documented by ASD, appearing as an exponential increase or decrease in the measured albedo in the UV/shortwave visible region, due to the instability of the VNIR detector. (Note that these measurements could often still be used for spectral analysis >976 nm, thus resulting in the higher N values for statistical analysis of these bands).

Finally, the remaining albedo measurements for each site were averaged, usually with 3–4 measurements used per site. After this initial

data processing, observations including weather field notes, the shape of the measured diffuse fraction curves, and signals of nearby irradiance sensors were used to determine the sky conditions at the time of the ASD measurements. Days with variable sky conditions were identified, and coinciding albedo measurements were eliminated for remaining days that showed especially high standard deviation between the four consecutive measurements and were obvious outliers in the time series. The resulting dataset is almost entirely high quality clear-sky measurements, but also includes ten days of entirely overcast measurements, and a small remainder of measurements in weakly variable sky conditions (often thin cirrus, haze, or diamond dust), that still showed high repeatability. After the QCQA procedure, there were approximately 40 days of data remaining (depending on the site and the bandwidths analyzed), out of 65 potential measurement days.

3. Results and discussion

3.1. ASD albedo time series

Fig. 4 shows selected bandwidth integrations for the ASD field-measured albedo time series for all five measurement sites, displaying one shortwave visible band (MODIS Band 3, 459–479 nm), one shortwave IR band (MODIS Band 5, 1230–1250 nm), and the broadband integration for the full spectral range of the instrument (350–2200 nm). An important feature of the time series for all of the bandwidths (including those not displayed) is the high correlation between the four fixed sites and the roving fifth site, and the constrained range of spatial variability displayed between all five sites. The five-site measurement technique provided an extensive dataset to quantify the spatial variability of albedo, both at the 4- to 15-meter scale among the four fixed sites, and at scales of 100 s of meters as the fifth site moved throughout and beyond the MODIS pixel, reaching maximum distances of 600–700 m from the four fixed sites. To examine spatial variability, the average daily range and the average daily standard deviation in albedo between the four fixed sites were analyzed for the entire campaign, and these values were found to negligibly increase with addition of the albedo measurements from the fifth roving site. For the broadband integration, the average range and average standard deviation for the four fixed sites are 0.019 and 0.009, respectively, and are 0.020 and 0.009, respectively, when the fifth roving stake is added. All seven narrowband integrations show very similar statistics between the five stakes, with the addition of the fifth stake never increasing the range or standard deviation of albedo more than 0.003 for any bandwidth. These results demonstrate that broadband albedo measured with a 2-meter radius field of view is, on average, within approximately 0.020 of albedo at any other location at both 10-meter and 100-meter scales of spatial variability.

3.2. Comparison to MODIS direct broadcast and v006 daily albedo

Figs. 5 and 6 show the time series plots of ASD field-measured albedo as an average of the four fixed sites, with MODIS albedo for the corresponding bandwidths. Fig. 5 shows the ASD broadband integration with the MODIS shortwave products, and Fig. 6 shows ASD and MODIS albedo for all seven narrow bandwidths. The spectral range of the MODIS shortwave bandwidth is considerably larger than that of the ASD measurements, however the shortwave product is very comparable to the ASD broadband integration, as there is very little downwelling solar energy represented above 2200 nm, or below 350 nm. MODIS Direct Broadcast low-quality flagged data are indicated in red, and high-quality flagged data are indicated in blue. The MODIS v006 dataset consists of only high quality data for the campaign period, and includes one period of missing data near the end of the campaign. As described in Section 2.5.3, the ASD measurements shown here represent the highest quality measurements of the campaign, with many individual

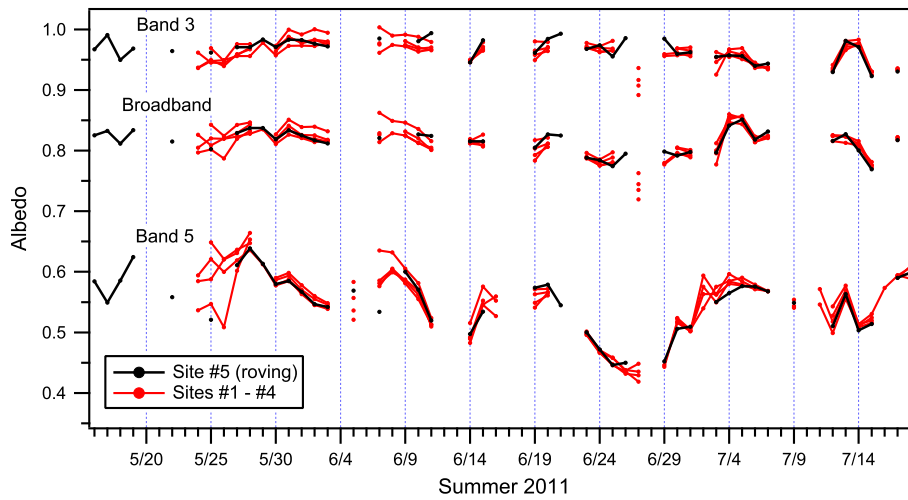


Fig. 4. Time series of ASD field-measured albedo at all five sites, for Band 3 (459–479 nm), Band 5 (1230–1250 nm), and Broadband (350–2200 nm) integrations.

points representing 16 consecutive albedo measurements (an average of 4 measurements at all 4 locations).

Figs. 5 and 6 show that the MODIS Direct Broadcast albedo is consistently lower in magnitude than the ASD field measurements, while the MODIS v006 albedo is much more tightly matched to the ASD measurements, at times both slightly lower and slightly higher than the ASD. Additionally, the ASD field measurements show much greater temporal variability over day to day and multiday periods, a consistent difference between field-measured albedo and MODIS albedo throughout the campaign.

Statistical results for all bandwidths between MODIS Direct Broadcast albedo and the ASD measurements are shown in Table 2, and corresponding results for the MODIS v006 albedo are shown in Table 3. In general, the MODIS products better match the ASD measurements at the shorter wavelength narrowbands, with the lowest values at Bands 3 and 4 for the Direct Broadcast product, and at Bands 4 and 1 for the v006 product. Maximum RMSE values are seen at Band 5 in both products, reflecting periods of high variability at these wavelengths in the field-measured albedo that create larger absolute differences from the MODIS albedo.

RMSE is a more representative error indicator in the case of this and previous studies, where datasets commonly show both positive and negative mean difference. The RMSE of 0.026 for MODIS v006 shortwave broadband albedo represents the lowest error value reported in a MODIS validation study (Table 4), indicating a significant improvement

from previous MODIS albedo products. Previous studies show RMSE values specifically for the Summit AWS of 0.035–0.037 (Stroeve et al., 2006), and 0.036 (Liang et al., 2005), however some RMSE values for the Summit AWS, and many for the entire AWS network range 0.040–0.075.

Although the MODIS albedo products are generally well matched in magnitude to the ASD albedo, with relatively low RMSE and mean difference values, the difference in temporal variability is very distinct, indicated in part by very low r^2 values. This relationship is also obvious in Table 5, showing the range of albedo (max. value–min. value) for all three time series, and in Table 6, showing the mean and standard deviation. The ASD measurements have a considerably greater range and standard deviation than both MODIS products, with the v006 product showing the lowest values, a somewhat unexpected result considering the emphasis on daily data in the v006 product. Also, it is observed that MODIS v006 Band 3 albedo occasionally reaches values >1.0 (up to 1.02), due to possible minor problems with the original surface reflectance atmospheric corrections, the MODTRAN simulated AODs, and/or the construction of the BRDF for that wavelength.

3.3. BSRN albedo measurements at Summit

Fig. 7 shows the BSRN albedo measurements for 1100 local Summit time (selected from 1-minute resolution data), along with the ASD broadband albedo and the two MODIS shortwave albedo products.

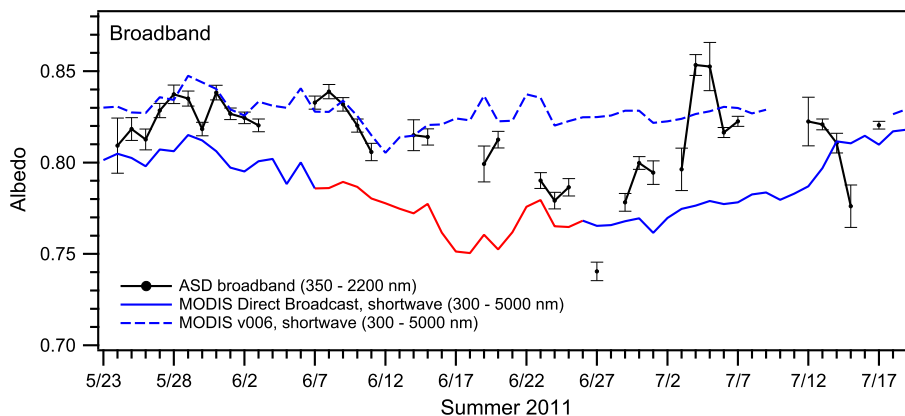


Fig. 5. Time series of ASD field-measured albedo, MODIS Direct Broadcast daily albedo, and MODIS v006 daily albedo, for the shortwave broadband. MODIS Direct Broadcast high-quality data is shown in blue, low-quality in red. All MODIS v006 albedo shown is high quality. ASD albedo is an average of the four fixed sites, with error bars representing the average standard deviation of the four sites, where standard deviation at a single site represents the variability between repeated measurements at that location.

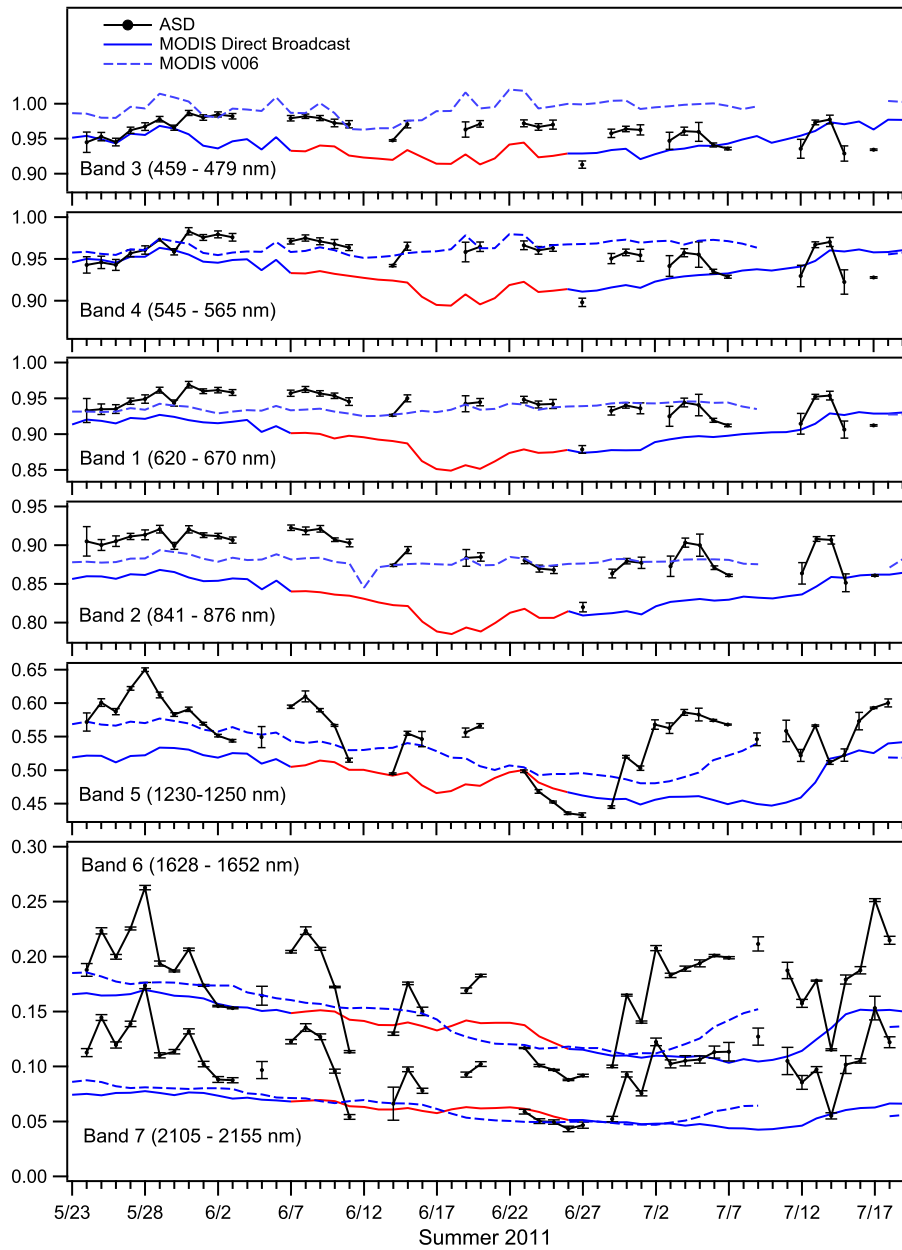


Fig. 6. Time series of ASD field-measured albedo, MODIS Direct Broadcast daily albedo, and MODIS v006 daily albedo, for MODIS Bands 1–7. MODIS Direct Broadcast high-quality data is shown in blue, low-quality in red. All MODIS v006 albedo shown is high quality. Left axis is albedo for all plots.

Table 2
Statistical results for MODIS Direct Broadcast albedo product vs. ASD albedo measurements (4-site average). N indicates the number of days with coinciding measurements.

MODIS band	Direct Broadcast (high-quality only)				Direct Broadcast (all data)			
	N	r ²	Mean difference	RMSE	N	r ²	Mean difference	RMSE
Broadband	25	0.136	0.023	0.033	37	0.168	0.027	0.035
Band 3	25	0.018	0.009	0.024	37	0.000	0.020	0.031
Band 4	25	0.138	0.010	0.022	37	0.011	0.020	0.031
Band 1	25	0.170	0.028	0.035	37	0.029	0.040	0.047
Band 2	25	0.392	0.045	0.050	37	0.277	0.055	0.059
Band 5	32	0.229	0.063	0.077	45	0.212	0.058	0.073
Band 6	32	0.138	0.045	0.059	45	0.130	0.037	0.054
Band 7	32	0.167	0.045	0.052	45	0.141	0.039	0.048

Table 3
Statistical results for MODIS v006 albedo product vs. ASD albedo measurements (4-site average). N indicates the number of days with coinciding measurements.

MODIS band	N	r ²	Mean difference	RMSE
Broadband	32	0.103	−0.015	0.026
Band 3	32	0.000	−0.030	0.036
Band 4	32	0.000	−0.007	0.021
Band 1	32	0.000	0.005	0.020
Band 2	32	0.216	0.012	0.025
Band 5	38	0.355	0.022	0.048
Band 6	38	0.258	0.026	0.045
Band 7	38	0.294	0.035	0.043

Table 4

Statistical results from previous MODIS snow albedo validation studies, shown with the broadband results of this study. Previous MODIS products/algorithms used include: MOD10A1 in Box et al. (2012) and Stroeve et al. (2006), MODSCAG in Painter et al. (2009), MOD43 in Stroeve et al. (2005), and DEA in Liang et al. (2005). GCNet AWS is the Greenland Climate Network Automatic Weather Stations, shown with the number of stations used.

Location (year)	N (days)	r ²	Mean difference	RMSE	MODIS quality flags	Reference
Summit (2011)	32	0.103	−0.015	0.026	high only	This study (v006)
Summit (2011)	25	0.136	0.023	0.033	high only	This study (Direct Brd.)
Summit (2011)	37	0.168	0.027	0.035	all	This study (Direct Brd.)
GCNet AWS (17) (2000–2010)	monthly (MJJA)	0.909	−0.009	0.041	N/A	Box et al. (2012)
San Juans, CO (2006)	30	–	0.036	0.042	all	Painter et al. (2009)
GCNet AWS (5) (2004)	158	0.624 (Terra)	–	0.067 (T)	all	Stroeve et al. (2006)
		0.593 (Aqua)		0.075 (A)		
Summit AWS (2004)	~55	–	–	0.035 (T)	all	Stroeve et al. (2006)
				0.037 (A)		
GCNet AWS (16) (2000–2003)	–	–	<0.020	0.040	high only	Stroeve et al. (2005)
	~175/yr	–	<0.020	0.070	all	
Summit AWS (2000–2003)	–	All-sky/BSA 0.253	0.027	0.065	all	Stroeve et al. (2005)
		All-sky/WSA 0.319	0.032	0.074		
		Clear-sky/BSA 0.135	0.020	0.061		
		Clear-sky/WSA 0.161	0.025	0.069		
Summit AWS (2000–2003)	–	–	−0.007	–	high only	Stroeve et al. (2005)
			0.003			
			−0.012			
			−0.012			
GCNet AWS (5) (2002)	~20	–	<0.02	0.04	all	Liang et al. (2005)
Summit AWS (2002)	~20	–	−0.005	0.036	all	Liang et al. (2005)

Table 7 demonstrates the relative magnitudes between the various albedo measurements, with the ASD and MODIS v006 albedo both showing low mean difference and RMSE values. However, the MODIS v006 albedo best matches the BSRN measurements, with an RMSE of 0.029, only slightly greater than the RMSE value comparing MODIS v006 albedo to ASD albedo (Table 3).

Perhaps the strongest confirmation of the ASD-measured temporal variability is the statistical results for the magnitude of temporal variability from the BSRN albedo time series, again demonstrating a much greater range of temporal variability than the MODIS results. Table 8 shows values for range and standard deviation that are almost matching between the ASD and BSRN measurements, and values that are considerably lower for the MODIS products. The range and standard deviation results for the BSRN time series were calculated with data only from coinciding days with the ASD measurements to prevent differences in atmospheric screening that could add an additional source of variability to the BSRN results. Even though the range of temporal variability is very similar between the two ground measurements, the poor correlation between the two time series could be a result of the difference in location: the BSRN station is located slightly less than 1 km from the ASD site, and it is likely seeing somewhat different snow conditions at any given time. It is also possible that the ASD sees a slightly different field of view than the BSRN station, which will change with snow depth over the season. However, the agreement

between the magnitude of ASD and BSRN variability is significant for the overall campaign goals, as the variability of the BSRN signal in part provided the motivation to investigate albedo variability at Summit.

3.4. DISORT modeled spectral albedo

The temporal variability of the ASD-measured albedo is additionally supported by radiative transfer modeling, using daily measurements of snow specific surface area, density, and chemistry (particularly dust and black carbon), as input to the DISORT code (Carmagnola et al., 2013). Those authors found that the field-measured spectral albedo on any day can be reproduced with an RMSE of 0.032. These results are consistent regardless of whether snow particulate absorbers (dust and BC) are included, demonstrating that the addition of impurities has a negligible effect on albedo at this location.

The model results provide support to the field measurements as an independent reproduction of the albedo time series. By using only inputs of snow physical properties, daily albedo spectrums are produced which closely match the measurements, giving particular support to the measured range of temporal variability, and providing evidence that most of the temporal variability of albedo is due to changes in snow physical properties, especially snow grain size. These results agree with observations of relatively low amounts of impurities

Table 5

Range (max. value–min. value) for the ASD 4-site average albedo and for the MODIS Direct Broadcast and v006 albedo time series.

MODIS band	Range (ASD)	Range (Direct Broadcast, high-quality only)	Range (Direct Broadcast, all data)	Range (v006)
Broadband	0.113	0.054	0.065	0.042
Band 3	0.074	0.054	0.061	0.037
Band 4	0.085	0.052	0.069	0.028
Band 1	0.091	0.057	0.082	0.021
Band 2	0.103	0.059	0.083	0.049
Band 5	0.217	0.087	0.087	0.097
Band 6	0.175	0.066	0.066	0.075
Band 7	0.130	0.035	0.035	0.040

Table 6

Mean and standard deviation for the ASD 4-site average albedo and for the MODIS Direct Broadcast and v006 albedo time series.

MODIS band	Mean, std. dev. (ASD)	Mean, std. dev. (Direct Broadcast, high-quality only)	Mean, std. dev. (Direct Broadcast, all data)	Mean, std. dev. (v006)
Broadband	0.814, 0.023	0.790, 0.017	0.784, 0.018	0.828, 0.008
Band 3	0.962, 0.018	0.947, 0.014	0.940, 0.016	0.993, 0.014
Band 4	0.956, 0.018	0.940, 0.015	0.932, 0.018	0.964, 0.007
Band 1	0.940, 0.019	0.906, 0.018	0.897, 0.022	0.936, 0.006
Band 2	0.891, 0.024	0.842, 0.019	0.833, 0.023	0.879, 0.007
Band 5	0.551, 0.050	0.490, 0.034	0.490, 0.028	0.529, 0.030
Band 6	0.174, 0.042	0.134, 0.025	0.136, 0.021	0.145, 0.024
Band 7	0.099, 0.030	0.059, 0.013	0.060, 0.011	0.064, 0.013

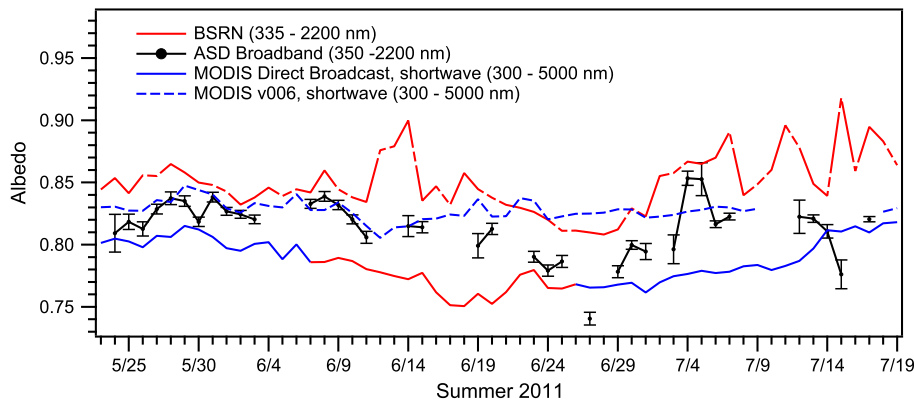


Fig. 7. Albedo time series for the BSRN station, the ASD broadband integration, and the MODIS Direct Broadcast and v006 shortwave products. MODIS Direct Broadcast high-quality data is shown in blue, low-quality in red. All MODIS v006 albedo shown is high quality.

in the snow at summit (Hagler, Bergin, Smith, & Dibb, 2007), and highest albedo variability observed in the ASD Band 5 integration, which is sensitive to changes in snow grain size of the near-surface. Bands 6 and 7 also show high variability (relative to the lower albedo at these wavelengths), additionally indicating the influence of snow grain size.

The link between snow physical properties and albedo is also observed in the field, where distinct albedo changes are often observed coinciding with distinct snow surface changes. It is common to see diurnal progressions such as the formation of abundant surface hoar or rime, that is then buffed into a layer of high density wind pack, that may then be covered by a layer of new snow precipitation (plates, columns, or dendrites). These sort of changes in the snow surface are thought to be largely responsible for the variability of albedo observed in both the ASD and BSRN measurements.

3.5. Possible sources of MODIS error

The MODIS values of “blue-sky” albedo for this study have been computed with a generalized aerosol optical depth, as opposed to actual coincident atmospheric measurements. It is therefore likely that some of the variability due to atmospheric effects as seen by the ASD field measurements is not being correctly captured in the MODIS values.

It is also possible that the MODIS albedo products lack the large temporal variability of the field measurements as a result of both the 16 day input required to build an accurate BRDF model, and the emphasis on all of the observations available over a single day to create the daily product, rather than focusing on observations specifically at the time of surface measurements. Even using both Aqua and Terra measurements, it is still necessary to use a 16-day period to have sufficient clear-sky, atmospherically corrected, multi-angular looks over the viewing hemisphere to adequately model the surface BRDF. The algorithm then emphasizes the measurements from a single day coupled with the generalized BRDF model, to better refine the albedo product by capturing the more subtle effects happening on a day to day basis. However, because the basic structure of the generalized BRDF is

utilizing the reflectance signals from 16 days of snow surface variability, the day to day variability likely becomes muted. Additional muting occurs by using all available observations on the single day of emphasis, which masks the maximum or minimum values that could be captured as a result of specific snow conditions that exist at the exact time of the surface measurements.

Even though we have demonstrated that a constrained albedo signal is measurable anywhere throughout the MODIS pixel, it still must be considered that MODIS is viewing over a 500-m resolution pixel. This larger scale of view could be affected by large-scale undulations in surface topography, and likely plays a role in the inability to capture changes due to snow crystal variability, which will dominate the ASD 2-meter radius field of view.

3.6. Spatial variability, surface slope effects, and surface roughness

Two spatial transect surveys were completed on May 17 and June 8 to measure the spatial variability of albedo, with measurements approximately every 50 m, moving 1.5 km east along the clean air sector boundary (Fig. 8). These surveys were completed near solar noon on clear sky days, attempting to eliminate the effects of solar zenith angle or variable diffuse light conditions. Only one measurement per location was completed on the May 17 survey, and the error bars on the June 8 survey represent one standard deviation of four repeated measurements at each location. The range, mean, and standard deviation of albedo for each survey are shown in Table 9.

It is unexpected that the range and standard deviation of albedo measured in the spatial surveys does not more closely match the scale of spatial variability present between the four fixed sites and the fifth roving site. Broadband spatial variability between the five measurement sites shows a range and standard deviation of 0.020 and 0.009, respectively, whereas the spatial surveys shows a range between 0.064 – 0.100, and standard deviation between 0.014 – 0.024. These surveys reach distances nearly twice as far from the fixed measurement site than was reached by the fifth roving stake, but the data from nearly two months of measurements at the five measurement sites shows that

Table 7

Statistics for the Baseline Surface Radiation Network albedo vs. the ASD broadband albedo measurements (4-site average), and vs. the MODIS shortwave albedo products. N indicates the number of days with coinciding measurements.

	N	r ²	Mean difference	RMSE
BSRN vs. ASD	37	0.142	0.036	0.045
BSRN vs. Direct Broadcast (high-quality only)	39	0.173	0.060	0.065
BSRN vs. Direct Broadcast (all data)	58	0.140	0.065	0.069
BSRN vs. v006	50	0.000	0.018	0.029

Table 8

Range (max. value–min. value), mean, and standard deviation for the BSRN albedo, for the ASD broadband albedo, and for the MODIS shortwave albedos. The values for BSRN are calculated only using coinciding days with the ASD measurements.

	Range	Mean, std. dev.
BSRN	0.108	0.850, 0.025
ASD broadband	0.113	0.814, 0.023
Direct Broadcast shortwave (high-quality only)	0.054	0.790, 0.017
Direct Broadcast shortwave (all data)	0.060	0.784, 0.018
v006 shortwave	0.042	0.828, 0.008

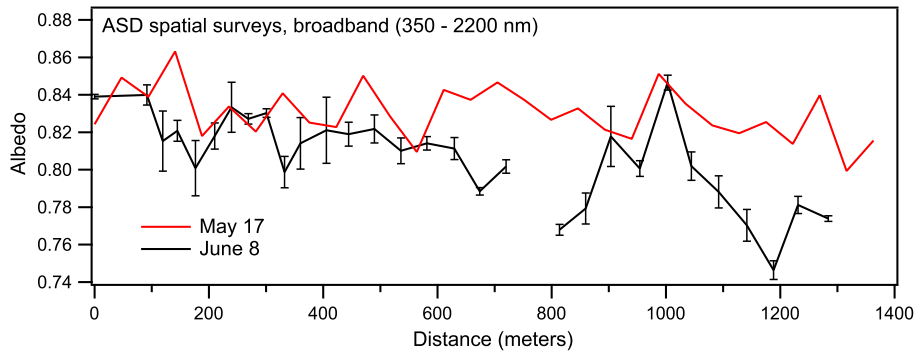


Fig. 8. ASD broadband albedo measurements from spatial surveys on May 17 and June 8. Measurements are approximately every 50 m, with one measurement per location on May 17 and 4 measurements per location on June 8 (error bars are 1 standard deviation of the repeated measurements).

albedo variability is largely constrained to scales less than 10 m. We would expect that the scale of albedo variability sampled with the fifth roving site would be quite similar to the variability measured at many hundreds of meters in the spatial transects. Because there were nearly 30 measurement locations in the spatial transects, and only 5 locations during daily measurements at the fixed sites, one could argue that we simply did not have enough measurement locations in the daily surveys to accurately represent spatial variability. However, if the larger range of variability represented by the spatial transects actually existed throughout the area of the long term sites, it seems very unlikely that this range of variability was never sampled over two months of randomly located measurements with the roving site, up to 700 m away.

The reasons for the difference in spatial variability are not entirely clear, however there are still important distinctions in the data between the scale of spatial variability and that of temporal variability in the ASD albedo time series. Although both spatial surveys display considerably larger variability than seen spatially among the five long-term sites, the range of temporal variability over the campaign is still greater (broadband value of 0.113), and it is also greater for most narrow bandwidths. This is especially true for Band 5 in the ASD time series, showing daily shifts in albedo of 0.075 and a total range of 0.217 over the course of the campaign, far greater than the range of spatial variability at any wavelength, and another strong indicator of the influence of snow grain size at these wavelengths. Bands 6 and 7 are also highly sensitive to changes in snow grain size, and similarly show high variability when analyzed relative to the lower albedo at these wavelengths. The dataset of the five long-term albedo sites is the campaign's largest density of measurements, and here we clearly see a pattern of a defined range of spatial variability at a given time, that moves through a greater range of temporal variability as surface conditions change.

There is some effect on the spatial variability data due to measurements on sloped surfaces, which at Summit are typically composed of small wind features that are meters in length and centimeters in height

(Albert & Hawley, 2002). Sloping surfaces can alter the measured albedo under clear skies, resulting in an apparent albedo that is different from the albedo of the flat surface. Using calculations presented in Grenfell et al. (1994), it is found that the effect of even a small sloped surface is significant: a 3° slope can show apparent albedos ranging from 0.90 of true albedo to 1.04 of true albedo. Although the effect of a sloped surface on apparent albedo is large given a consistent surface, the actual effect on our field measurements with the slope angles encountered at Summit is likely less than this. If features are generally small in relation to the instrument field of view, and are randomly distributed across an otherwise very flat surface, it is unlikely that the upwelling measurements would receive the majority of the cosine response from a significantly sloped or consistently sloped surface. The occurrence of small but consistent slope angles (0.5°–1°) over longer distances may also be possible, and this could have a larger effect on albedo measurements. In Albert and Hawley (2002), surface geometries were measured that were judged to be characteristic of the surrounding terrain, but precise surface geometries at Summit have not been entirely surveyed in detail at different spatial scales, so it is difficult to know the exact magnitude of inaccuracy in our measurements due to surface slope effects.

However, the spectral signals of the spatial surveys tend to indicate a significant surface slope effect: these surveys show variability in range and standard deviation that is very similar in magnitude across all bandwidths. Apparent albedo due to surface slope will tend to shift albedo measurements uniformly across the entire measured spectrum (Grenfell et al., 1994), and this is the pattern we observe in the spatial survey data. In the May 17 survey, there is still a maximum in spatial variability at Band 5, indicating that grain size is playing some role in the measured variability, but this relationship is not seen in the June 8 survey.

It is an important distinction that we suspect potential error is due to surface slope, as opposed to sastrugi shadowing effects such as those discussed. The surface patterns at Summit are not large enough or consistent enough to be considered true sastrugi, and the surface features rarely produce significant shadows unless the solar zenith angle is very large. Besides slight surface slopes as discussed above, surface roughness at Summit largely consists of textural differences between, for example, wind scoured and wind drifted snow, and the resulting impact on albedo measurements is captured by measurements of snow specific surface area variability.

Table 9

Range (max. value – min. value), mean, and standard deviation for ASD albedo spatial surveys on May 17 and June 8, 2011.

MODIS band	May 17 spatial survey		June 8 spatial survey	
	Range	Mean, std. dev.	Range	Mean, std. dev.
Broadband	0.064	0.830, 0.014	0.100	0.807, 0.024
Band 3	0.057	0.977, 0.013	0.118	0.949, 0.024
Band 4	0.068	0.969, 0.014	0.133	0.942, 0.028
Band 1	0.071	0.955, 0.015	0.135	0.929, 0.029
Band 2	0.075	0.918, 0.017	0.119	0.887, 0.030
Band 5	0.087	0.583, 0.022	0.084	0.581, 0.023
Band 6	0.048	0.211, 0.012	0.035	0.203, 0.009
Band 7	0.032	0.135, 0.008	0.017	0.121, 0.005

4. Conclusions

We have analyzed ASD spectral albedo measurements completed at Summit Station, Greenland during May, June, and July of 2011, and compared these results to both the MODIS v005 Direct Broadcast daily albedo, and the MODIS v006 MCD43A daily albedo products. Analyzing MODIS v005 Direct Broadcast, high-quality only retrievals, Root Mean

Square Error (RMSE) for the shortwave broadband albedo is 0.033, and the narrow bandwidths range 0.022–0.077. The MODIS v006 albedo product shows considerable improvement over previous albedo products, with shortwave broadband RMSE of 0.026, and narrow bandwidths ranging 0.020–0.048. The new Version 006 albedo also shows improvement in reported error values from previous MODIS field validations in Greenland, which have been limited to broadband data from the Greenland Climate Network Automatic Weather Stations.

In comparison to ASD field measurements, the MODIS v005 Direct Broadcast product is consistently lower in magnitude across all bands, and the improved Version 006 product is less biased, showing albedo both slightly lower and slightly higher than field measurements. However, the MODIS products do not show similar trends in the magnitude of temporal variability as measured on the surface. The ASD measurements show much greater variability on day to day and multi-day scales, with the broadband ASD albedo ranging 0.113 over the course of the campaign, commonly with daily shifts up to 0.060. ASD albedo integrated for Band 5 (1230–1250 nm) shows the greatest amount of variability, ranging 0.217 over the campaign with daily shifts up to 0.075. This maximum in albedo variability at Band 5 demonstrates the control of snow grain size at these wavelengths, which is additionally supported by the variability at Bands 6 and 7, also highly variable relative to the lower albedo at these wavelengths. MODIS may be inaccurately representing the range of temporal variability due to both the 16-day construction of the generalized BRDF in the BRDF/albedo algorithm, and due to the utilization of all observations available on a single day when comparing to surface measurements made at one particular time of day. Also, the MODIS values have been derived using only a generalized aerosol model, which likely does not capture the variability due to actual aerosol conditions as measured from the surface.

The range of temporal variability in the ASD spectral albedo measurements is in agreement with albedo measurements at the Baseline Surface Radiation Network (BSRN) station at Summit, although the timing of these variations differ, likely a result of the spatial separation between the two sites and differences in field of view. The range and standard deviation for coinciding measurement days between the two instruments are within 0.005 and 0.002, respectively. The ASD measurements show an RMSE with the BSRN station of 0.045, and the MODIS v006 albedo product shows an even better match to the BSRN measurements with an RMSE of 0.029.

The high temporal variability of the ASD measurements is also supported by modeled albedo results presented in Carmagnola et al. (2013). Modeled spectral albedo produced using the DISORT code, coinciding with each day of ASD measurements, and using daily measurements of snow specific surface area, density, and chemistry as model inputs, are shown to reproduce field-measured albedo with an RMSE of 0.032.

An analysis of four fixed measurement sites and a fifth roving site shows a defined range of spatial variability that exists throughout the 500-meter resolution MODIS pixel, with the range in broadband albedo averaging 0.020 for the campaign. The four fixed sites are representative of 4–15 meter variability, whereas the fifth roving site represents measurements up to 700 m away. Addition of albedo measurements from the fifth site does not significantly increase the range or standard deviation of spatial variability measured among the four fixed sites. The temporal pattern of the measurement sites shows a limited range of spatial variability that moves through a considerably greater range of temporal variability as surface snow conditions change on day to day and multiday scales.

This work confirms the temporal variability of albedo measured by the BSRN station at Summit, which has important implications for the radiative balance over central Greenland. Although the MODIS daily albedo products do not capture the range of temporal variability as measured with the ASD on the surface, the v006 MODIS product is in considerably better agreement with surface measurements than previous studies, providing increased potential for the use of remotely sensed

albedo to aid in calculations of atmospheric and surface processes over the Greenland ice sheet.

Future work should include more extensive surface measurements of the spatial variability of albedo, as well as a detailed analysis of the surface geometries of the ice sheet to analyze the effects of surface slope on albedo. Additionally, the v006 MODIS daily albedo algorithm should be improved to even better emphasize the single day of interest within the 16-day period used in the BRDF/albedo algorithm, potentially gaining an ability to emphasize measurements made at a particular time within a single day.

Acknowledgements

We would like to acknowledge the support of NSF Office of Polar Programs who in part supported this work (Grant Number 1023227). Crystal Schaaf and Zhuosen Wang acknowledge support from NASA MODIS grant NNXAL38G. The authors also wish to thank: Brandon Strellis, Hannah James, Ryan Schilling, and Chelsea Corr for assistance with the daily ASD albedo measurements; Don Perovitch at CRREL for loan of the ASD instrument; R. Brandt, T. Grenfell, S. Hudson, and S. Warren for discussion of shadow and cosine corrections; H. Rodstein at Wavemetrics for software support. Much thanks to the support crew at Summit Station, and to the 109th Air National Guard.

References

- Albert, M. R., & Hawley, R. L. (2002). Seasonal changes in snow surface roughness characteristics at Summit, Greenland: implications for snow and firn ventilation. *Annals of Glaciology*, 35(1), 510–514.
- Box, J. E., Fettweis, X., Stroeve, J. C., Tedesco, M., Hall, D. K., & Steffen, K. (2012). Greenland ice sheet albedo feedback: thermodynamics and atmospheric drivers. *The Cryosphere*, 6, 821–839. <http://dx.doi.org/10.5194/tc-6-821-2012>.
- Carmagnola, C. M., Domine, F., Dumont, M., Wright, P., Strellis, B., Bergin, M., et al. (2013). Snow spectral albedo at Summit, Greenland: comparison between in situ measurements and numerical simulations using measured physical and chemical properties of the snowpack. *The Cryosphere*, 7, 1139–1160. <http://dx.doi.org/10.5194/tc-7-1139-2013>.
- Donohoe, A., & Battisti, D. S. (2011). Atmospheric and Surface Contributions to Planetary Albedo. *Journal of Climate*, 24(16), 4402–4418.
- Grenfell, T. C., Warren, S. G., & Mullen, P. C. (1994). Reflection of solar radiation by the Antarctic snow surface at ultraviolet, visible, and near-infrared wavelengths. *Journal of Geophysical Research*, 99(D9), 18,669–18,684.
- Gallet, J. C., Domine, F., Zender, C. S., & Picard, G. (2009). Rapid and accurate measurement of the specific surface area of snow using infrared reflectance at 1310 and 1550 nm. *The Cryosphere Discussions*, 3(1), 33–75.
- Hagler, S. W., Bergin, M. H., Smith, E. A., & Dibb, J. E. (2007). A summer time series of particulate carbon in the air and snow at Summit, Greenland. *Journal of Geophysical Research*, 112(D21309). <http://dx.doi.org/10.1029/2007/JD008993>.
- Liang, S., Stroeve, J., & Box, J. E. (2005). Mapping daily snow/ice shortwave broadband albedo from Moderate Resolution Imaging Spectroradiometer (MODIS): the improved direct retrieval algorithm and validation with Greenland in situ measurement. *Journal of Geophysical Research*, 110, D10109. <http://dx.doi.org/10.1029/2004JD005493>.
- Liu, J., Schaaf, C., Strahler, A., Jiao, Z., Shuai, Y., Zhang, Q., et al. (2009). Validation of Moderate Resolution Imaging Spectroradiometer (MODIS) albedo retrieval algorithm: dependence of albedo on solar zenith angle. *Journal of Geophysical Research*, 114, D01106. <http://dx.doi.org/10.1029/2008JD009969>.
- Lucht, W., Schaaf, C. B., & Strahler, A. H. (2000). An algorithm for the retrieval of albedo from space using semiempirical BRDF models. *Geoscience and Remote Sensing, IEEE Transactions*, 38(2), 977–998.
- Painter, T. H., Rittger, K., McKenzie, C., Slaughter, P., Davis, R. E., & Dozier, J. (2009). Retrieval of subpixel snow covered area, grain size, and albedo from MODIS. *Remote Sensing of Environment*, 113(4), 868–879.
- Román, M.O., Schaaf, C. B., Lewis, P., Gao, F., Anderson, G. P., Privette, J. L., et al. (2010). Assessing the coupling between surface albedo derived from MODIS and the fraction of diffuse skylight over spatially-characterized landscapes. *Remote Sensing of Environment*, 114(4), 738–760.
- Schaaf, C. B., Gao, F., Strahler, A., Lucht, W., Li, X., Tsang, T., et al. (2002). First operational BRDF, albedo nadir reflectance products from MODIS. *Remote Sensing of Environment*, 83, 135–148.
- Schaaf, C. B., Wang, Z., & Strahler, A. (2011). Commentary on Wang and Zender-MODIS snow albedo bias at high solar zenith angles relative to theory and to in situ observations in Greenland. *Remote Sensing of Environment*, 115, 1296–1300.
- Steffen, K., Box, J. E., & Abdalati, W. (1996). Greenland climate network: GCNet, US ARMY Cold Regions Research and Engineering (CRREL). *CRREL Special Report* (pp. 98–103).
- Stroeve, J., Box, J. E., Gao, F., Liang, S., Nolin, A., & Schaaf, C. (2005). Accuracy assessment of the MODIS 16-day albedo product for snow: comparisons with Greenland in situ measurements. *Remote Sensing of Environment*, 94(1), 46–60.

- Stroeve, J. C., Box, J. E., & Haran, T. (2006). Evaluation of the MODIS (MOD10A1) daily snow albedo product over the Greenland ice sheet. *Remote Sensing of Environment*, 105(2), 155–171.
- Vermote, E. F., & El Saleous, N. Z. (2006). Operational atmospheric correction of MODIS visible to middle infrared land surface data in the case of an infinite Lambertian target. In J. Qu (Ed.), *Earth Science Satellite Remote Sensing, Science and Instruments, Vol. 1.* (pp. 123–153) New York: Springer Berlin Heidelberg.
- Vermote, E. F., El Saleous, N. Z., & Justice, C. O. (2002). Atmospheric correction of MODIS data in the visible to middle infrared: first results. *Remote Sensing of Environment*, 83(1–2), 97–111.